Cement and Concrete Research 41 (2011) 301–310

Contents lists available at ScienceDirect

Cement and Concrete Research

journal homepage: http://ees.elsevier.com/CEMCON/default.asp

Influence of activator type on hydration kinetics, hydrate assemblage and microstructural development of alkali activated blast-furnace slags

M. Ben Haha *, G. Le Saout, F. Winnefeld, B. Lothenbach

Empa, Swiss Federal Laboratories for Materials Science and Technology, Laboratory for Concrete and Construction Chemistry, Ueberlandstrasse 129, 8600 Dübendorf, Switzerland

ARTICLE INFO

Article history:
Received 24 August 2010
Accepted 23 November 2010

Keywords:
Alkali Activated Cement (D)
Microstructure (B)
Calcium-Silicate-Hydrate (C-S-H) (B)
Image Analysis (B)
Mechanical Properties (C)

ABSTRACT

The hydration of two slags with different Al_2O_3 contents activated with sodium hydroxide and hydrous sodium metasilicate (commonly named water glass) is studied using a multi-method approach. In all systems, C-S-H incorporating aluminium and a hydrotalcite-like phase with Mg/Al ratio ~2 are the main hydration products. The C-S-H gels present in NaOH activated pastes are more crystalline and contain less water; a calcium silicate hydrate (C-S-H) and a sodium rich C-N-S-H with a similar Ca content are observed at longer hydration times. The activation using NaOH results in high early strength, but strength at 7 days and longer is lower than for the sodium metasilicate systems. The drastic difference in C-S-H structure leads to a coarser capillary porosity and to lower compressive strength for the NaOH activated than for the sodium metasilicate activated slags at the same degree of slag reaction.

1. Introduction

In order to reduce the CO_2-emissions related to cement manufacturing, the application of industrial by-products rich in aluminium and silicon oxide in alkaline activated binders is a promising option [1,2]. Materials generally used are blastfurnace slag, fly ash or metakaolin, which are activated by the addition of alkalis like alkali silicates or hydroxides [3–6].

Alkali activated slags (AAS) can have high strength development and using the adequate activators can lead to rapid setting, good durability and high resistance to chemical attack [2–8]. The main hydration products found in AAS are C-S-H with a low Ca/Si ratio related mainly to the composition of the slag and the nature of activators used, hydrotalcite intimately intermixed with the C-S-H in the MgO containing slag and in some cases also an AFm phase, most probably strätlingite [9–13]. The C-S-H produced by alkali activated systems may incorporate a higher content of Al_2O_3 based on the initial composition of the slag [12,14,15]. Many variables influence the reaction of alkali activated slags such as fineness, chemical composition, water/binder (w/b) ratio, temperature or the pH [16–23]. A better understanding of the effects of alkaline activators such as NaOH and hydrous sodium metasilicate ($Na_2SiO_3 \cdot 5H_2O$) on the hydration mechanisms of alkali activated slag could indicate ways to optimise the use of alkaline activators.

An important factor that influences the porosity and thus the compressive strength is the kinetics of the hydration. In Portland cement systems it has been observed that a fast initial reaction as e.g. caused by elevated temperatures or accelerators, results in the formation of a dense hydration product and less reduction of the initial porosity that affects adversely the mechanical properties at later ages [24,25].

This paper investigated the major hydration products formed in alkali activated slags and their composition, morphology and spatial distribution. The study was carried out using two slags with different Al_2O_3 content to investigate the influence of the slag composition on the types of hydrates formed. An image analysis method was adopted to quantify the degree of hydration and the amount of coarse porosity directly from the backscattered electron (BSE) image of polished slag pastes samples. By studying the coarse porosity and degree of hydration using different alkaline activators, the relationship between microstructural properties and compressive strength was established.

2. Materials and experiments

Two ground granulated blast furnace slags (GGBFS) with different Al_2O_3 contents were studied: GGBFS LA exhibits a low Al_2O_3 content of 7.1 wt.%, and GGBFS HA a higher content of 12.0 wt.% Al_2O_3 (Table 1) with a similar particle size distribution. Two types of activators were used: NaOH and hydrous sodium metasilicate $Na_2SiO_3 \cdot 5H_2O$ (labeled here as NSH_5 and commonly referred to as water glass). The dosage of both activators and the amount of water were selected to obtain the same Na_2O content and water content in the two systems. The activators were dissolved in the water prior to the mixing in order to have a homogeneous distribution. The compositions of the pastes are presented in Table 2. All pastes were

* Corresponding author. Tel.: +41 44 823 49 47; fax: +41 44 823 40 35.
E-mail address: mohsen.ben-haha@empa.ch (M. Ben Haha).

0008-8846/$ – see front matter © 2010 Elsevier Ltd. All rights reserved.
doi:10.1016/j.cemconres.2010.11.016

Table 1
Chemical composition (oxides in wt.%) of the GGBFS.

	GGBFS HA	GGBFS LA
SiO_2	37.4	41.2
Al_2O_3	**12.0**	**7.1**
Fe_2O_3	0.58	1.0
CaO	36.5	39.4
MgO	8.0	7.4
SO_3	2.4	1.6
K_2O	1.2	0.7
Na_2O	0.40	0.57
TiO_2	0.50	0.26
Mn_2O_3	1.6	1.1
P_2O_5	0.03	<0.01
C:S	0.98	0.96
Loi	−0.41	−0.98
Ca/Si (atomic)	1.05	1.03
Mg/Al (atomic)	1.7	2.7

Loi: loss on ignition.

hydrated at 20 °C in closed plastic vessels to avoid the loss of water and ingress of CO_2.

Compressive strength measurements were undertaken in duplicate pastes samples with the dimension 25 mm × 25 mm × 25 mm cut from the samples hydrated in the sealed plastic vessels.

Crushed paste samples were used to perform thermogravimetric analysis (TGA) and X-ray diffraction (XRD). The hydration was stopped using solvent exchange with isopropanol.

A Mettler-Toledo simultaneous thermal analysis apparatus (TGA/SDTA 851) was used for TGA. The samples were heated from 30 °C to 980 °C in aluminium oxide crucibles with a heating rate of 20 K/min under N_2.

XRD data were collected using a PANalytical X'Pert Pro MPD diffractometer in a θ–2θ configuration using incident beam monochromator with CuKα radiation (λ = 1.54 Å). The samples were scanned between 5° and 70° 2θ with the X'celerator detector. The Rietveld analysis of amorphous slag has been done using X'Pert High Score Plus program from PANalytical (version 2.1). The amount of amorphous material in anhydrous slags was deduced by using the spiking method with 10 wt.% of CaF_2 as internal standard [26].

Slices of the hydrated samples were also examined by scanning electron microscopy (Philips ESEM FEG XL 30) using backscattered electron images (BSE) and energy-dispersive X-ray spectroscopy microanalysis (EDX) to determine the ratios of the different elements in the matrix on polished samples (more than 100 points are taken for each measurement). For the BSE study, the samples were cut into 1–2 mm thick slices. The hydration was stopped using solvent exchange by immersing the slices in isopropanol. The slices were further impregnated with epoxy resin, polished to 1/4 μm and coated with carbon.

Scanning electron microscopy image analysis (SEM-IA) was used to determine the degree of hydration of slag as well as the amount of coarse porosity of the hydrated slag pastes. The technique uses the grey level histogram segmentation to determine the different species observed in a BSE image [27–31]. The sensitivity of BSE to the chemical composition of the analyzed materials leads to the phase contrast in the grey level histogram observed in BSE images. The higher the average atomic number of a phase, the higher the number of generated BSE, and consequently the brighter the phase will appear in the image. Therefore, the different phases can be distinguished due to the intensity of BSE emitted, which results in a difference in their grey level on the acquired images. The densest phases are the brightest (mainly unreacted slag) whereas less dense phases are the darkest in the image (corresponding mainly to porosity). The reaction of the anhydrous slag is measured by comparing the volume of anhydrous slag in the hydrated pastes with the slag content in the unhydrated pastes prior to the mixing. The measurement uncertainty is based on the threshold and edge detection as well as the effect of presence of initial porosity within the mixes is around 2–3%. The volume of coarser pores as determined by SEM-IA includes, depending on the magnification (2500×) used, pore sizes in the range of 0.1 to 5 μm and is referred to as "coarse porosity" in this paper. The uncertainty in the case of porosity is lower since it includes only the threshold uncertainties and is within 0.5 to 1%.

Table 2
Mix composition of the slag pastes (weight ratios relative to 100 g slag).

Formulation	Binder		Water
	Slag	Activator	
NaOH	100	3.9	41.6
NSH_5	100	11.1	39.7

Table 3
Compressive strengths (MPa) of the paste samples.

Age (day)	HA		LA	
	NaOH	NSH_5	NaOH	NSH_5
1	8.3	n.a	6.2	n.a
7	15.9	25.7	19.3	20.4
28	24.2	44.4	22.1	36.5
90	27.4	52.1	25.2	44.2
180	30.9	61.1	28.2	56.2

n.a: not analyzed.

The development of compressive strength is linked to the degree of reaction, the microstructure, the kind and amount of solids present and the coarse porosity. The degree of reaction can be determined: (i) indirectly by TGA by measuring the amount of hydrates formed; and (ii) directly by measuring the disappearance of the anhydrous slag by SEM image analysis technique (SEM-IA).

3. Results and discussions

3.1. Strength development

Depending on the activators used, the development of the compressive strengths differs (Table 3). NaOH as activator gives a high compressive strength already after 1 day. In contrast, the NSH_5 activated pastes have no measurable compressive strength after 1 day, but the compressive strength after 7 days is higher than for the NaOH activated slags. After 180 days, the compressive strength of the NSH_5 activated slags is twice as high as the strength of the NaOH activated slags. The samples activated with NSH_5 gain approximately 70–80% in compressive strength between 7 days and 28 days and more than double after 180 days with respect to 7 day samples for both slags. The activation with NaOH leads at later ages to little further development of the compressive strength (see Fig. 1).

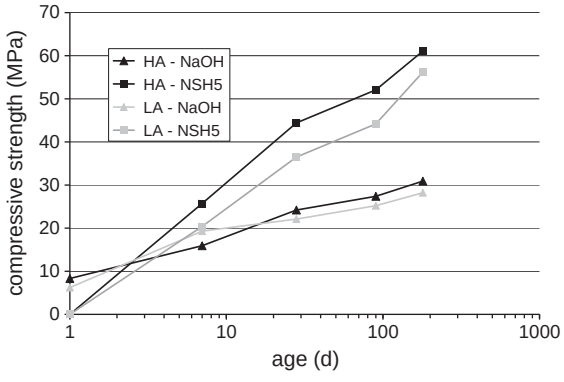

Fig. 1. Compressive strength development in the different alkali activated systems.

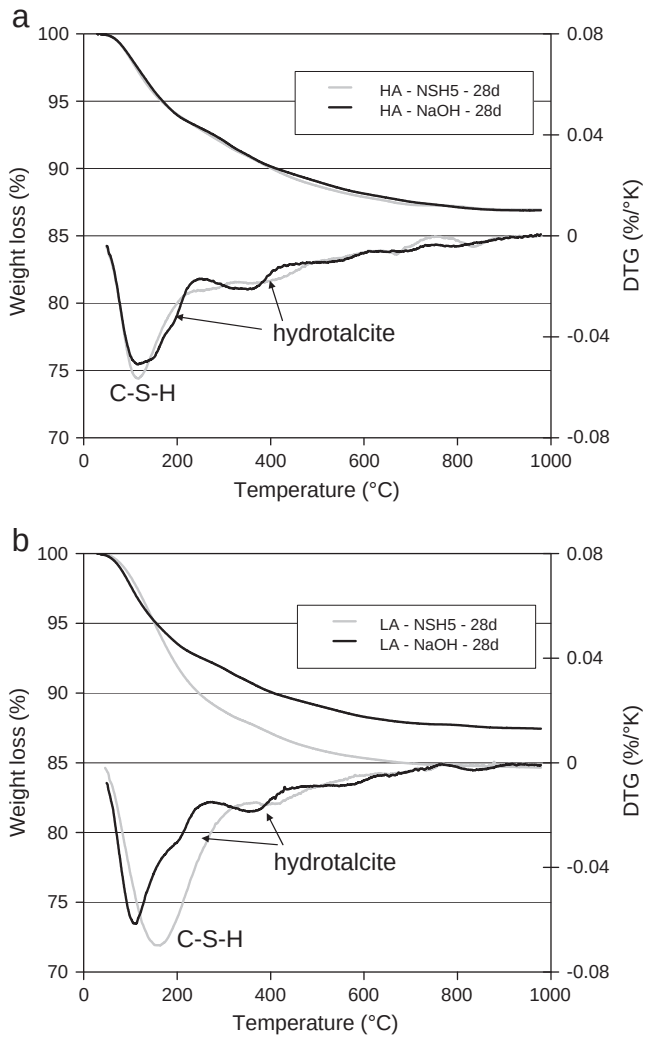

Fig. 2. Thermogravimetric analyses (TGA and DTG) of alkali activated systems of both slags at 28 days (a) HA slag, and (b) LA slag.

Both activated high aluminium HA slags show a slightly higher compressive strength at almost all ages than the LA slags. The difference in compressive strength is significant for the NSH_5 activated slags (~20%) while the effect is small for the NaOH activated slags (~10%).

3.2. Thermogravimetric analysis (TGA)

The TGA data as given in Fig. 2 indicate the presence of C-S-H (main weight loss 50–200 °C) and hydrotalcite-like phases. The hydrotalcite-like compound has a layered structure and is also designated as layered double hydroxides (LDHs). The formula is represented by $Mg^{2+}{}_xAl^{3+}{}_y(OH)^-{}_{2(x+y)}(CO_3)^{2-}{}_{y/2}\ mH_2O$. Structurally, the hydrotalcite-like compound consists of two dimensional brucite-like layers with positive charge, where the cations are located in the center of an octahedron surrounded by six hydroxyl groups, and anions together with water molecules are arranged in the interlayer to form neutral materials. This compound will be named here hydrotalcite and labeled in the text Ht (weight loss at around 200 °C and 400 °C) [32,33]. Both, C-S-H and hydrotalcite phase are generally observed in hydrated AAS [8,10,12,34,35]. The weight losses at 200 and 400 °C associated with hydrotalcite are more distinct for HA than for LA.

The total loss of weight up to 600 °C is a relative measure of the degree of hydration in systems with a similar phase assemblage [36,37].

Table 5 summarises the different weight losses from 30 to 600 °C. The use of NaOH as activator results in a fast hydration during the first day. In the NSH_5 activated slag systems, the early hydration proceeds more slowly than in the NaOH activated systems. However, after 28 days and longer, the weight losses of NSH_5 activated slags are higher. Also the bound water content (Table 5) and the volume of the hydration products are lower for the NaOH activated slags than for the NSH_5 activated slags. This is consistent with the finding of a previous study [36], where less water in the reaction products of NaOH was observed than of NSH_5 activated slags.

Activated with NaOH, the HA slag shows a higher content of bound water than LA at 28 days and beyond, whereas up to 7 days the opposite is the case. With NSH_5, both slags show roughly the same content of bound water, independent from the sample age.

3.3. Hydrates assemblage

3.3.1. X-ray diffraction

The X-ray diffractogramm of the raw LA slag (Fig. 3) present a hump around 29° due to the presence of amorphous phase. We can also observe the presence of akermanite $Ca_2(Mg, Al)(Si, Al)_2O_7$ and hatrurite (Ca_3SiO_5) inclusions. The amount of amorphous in both slags deduced by XRD is around 95 wt.%.

The hydrated samples show besides the background hump related to the unhydrated slag additional reflections at 29° and 49.5°, which can be attributed to C-S-H [8]. In the NaOH activated system, an additionally basal reflection at 7° 2θ is observed and also a less broad

Table 4
Atomic ratios observed in the hydration products by EDX-analyses.

Activators	NaOH								NSH_5			
Hydrates	C-S-H I (bright zone)			Ht	C-N-S-H (dark zone)			Ht	C-S-H			Ht
Ratio	Ca/Si	Na/Si	Al/Si	Mg/Al	Ca/Si	Na/Si	Al/Si	Mg/Al	Ca/Si	Na/Si	Al/Si	Mg/Al
HA												
1 day	0.89	0.12	0.23	2.15	–	–	–	–	–	–	–	–
7 days	0.90	0.12	0.23	2.12	–	–	–	–	0.79	0.12	0.22	2.09
28 days	0.88	0.12	0.23	2.09	–	–	–	–	0.79	0.12	0.22	2.05
180 days	0.91	0.12	0.23	2.14	0.89	0.61	0.23	2.12	0.82	0.13	0.21	2.09
LA												
1 day	0.88	0.13	0.14	2.11	–	–	–	–	–	–	–	–
7 days	0.92	0.12	0.14	2.10	–	–	–	–	0.77	0.13	0.13	2.01
28 days	0.91	0.12	0.14	2.09	–	–	–	–	0.78	0.13	0.14	2.10
180 days	0.91	0.12	0.14	2.07	0.92	0.64	0.15	2.01	0.81	0.12	0.13	2.07

Table 5
Weight loss from TGA (30–600 °C) in wt.% of the hydrated alkali activated slags.

Age (day)	HA		LA	
	NaOH	NSH_5	NaOH	NSH_5
1	8.5	4.7	7.9	5.7
7	9.3	7.7	10.1	7.1
28	13.1	13.1	11.7	12.8
90	15.2	16.2	12.2	15.2
180	15.7	17.3	13.3	17.2

reflection at 29° 2θ (Fig. 3) that match with the powder diffraction file of C-S-H (I) (PDF 034-0002) with a similar Ca/Si ratio around 1 (referred later as C-N-S-H). The basal reflection (7° 2θ) and narrow peak indicate a C-S-H with a more pronounced nanometric size of the coherent domain. The basal reflection represents the layer thickness of a 3D structural ordering in the C-S-H. However, the link of the observed features with the composition of the C-S-H is not straightforward as this basal peak can be observed in C-S-H with Ca/Si from 0.2 to 1.7 [38,39] as well in alkali silicate gels [40] and thus cannot be linked with a particular Ca/Si ratio. The two different peaks at around 29° 2θ represent the b unit cell parameter (within the layer) of the C-S-H. The difference in the unit cell parameters of these two C-S-H,

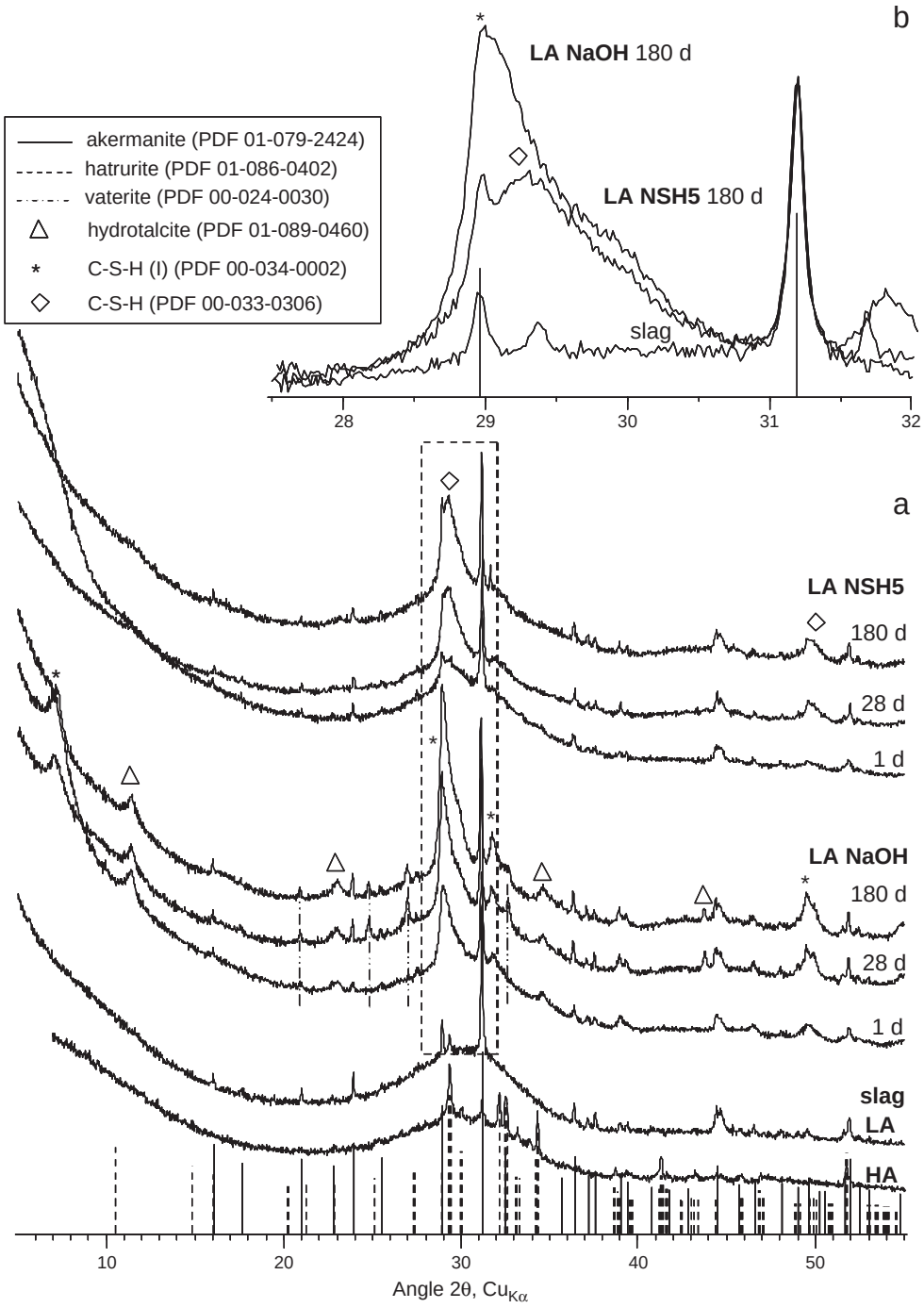

Fig. 3. XRD patterns of HA and LA unreacted slag and LA slag at different ages with NaOH and hydroussodium metasilicate (NSH_5) (a). The upper figure (b) shows detailed view between 27 and 32°.

present in the paste activated with NaOH, reveals two C-S-H with possibly different densities.

In the pastes activated with NaOH, reflections corresponding to hydrotalcite are present after one day, whereas even after 6 months such reflections cannot be clearly identified in the NSH_5 activated pastes (this is in agreement with an earlier study [12]). We can also notice some trace of vaterite in the LA Na(OH) sample probably due to some carbonation.

The observed diffraction patterns of the HA slag do not differ significantly from the LA slag, thus only LA slag is shown in Fig. 3.

3.3.2. EDX microanalyses

In the SEM observations (see Figs. 4–6) combined with EDX microanalyses, three types of hydrate phases could be identified: C-S-H, a C-S-H with high Na content (C-N-S-H) only occurring in the NaOH activated slags as well as hydrotalcite. Table 4 presents the main elemental ratios of these phases as derived from EDS point analyses.

The C-S-H formed in the presence of NaOH or NSH_5 has a Ca/Si ratio from 0.6 to 1.4 (Table 4) with a mean Ca/Si ratio of 0.9 (NaOH) and 0.8 (NSH_5). This corresponds to previously reported values for similar systems [8,11,12,14,36,41]. The Ca/Si ratios observed in the NSH_5 activated slags show a lower Ca/Si level, possibly due to the presence of additional Si from the NSH_5 activator. The Al/Si ratio of the C-S-H is similar for both activators.

In the NaOH activated slags two different C-S-H phases can be observed after longer hydration times, a brighter outer zone that is formed during the first days of hydration and an inner darker zone that forms at later hydration times (Fig. 5). The Al/Si and Ca/Si ratios of the C-S-H in the dark zone are similar to those in the bright zone but

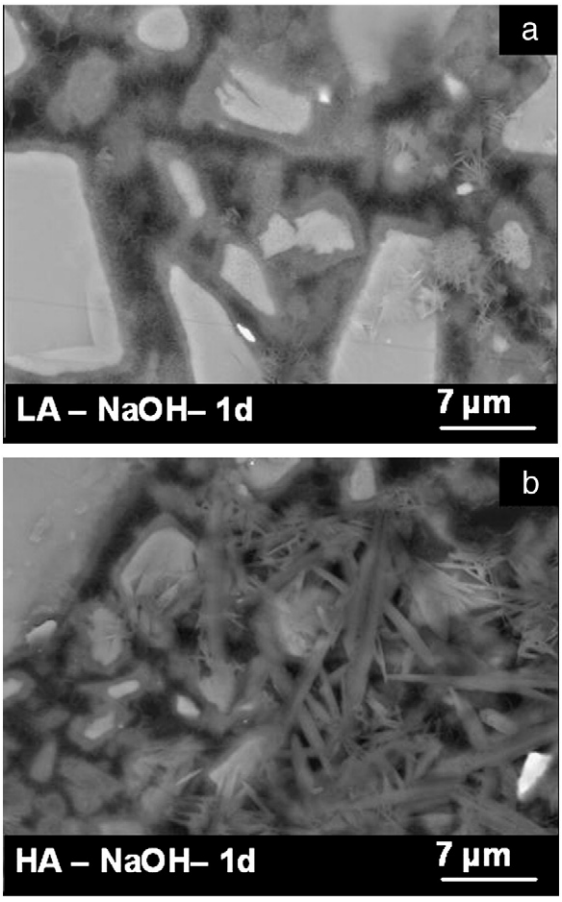

Fig. 4. Microstructure of NaOH activated slag after 1 day showing C-S-H layer around the slag particles as well as platelets of hydrotalcite. (a) LA slag with NaOH after 1 day, and (b) HA slag with NaOH after 1 day.

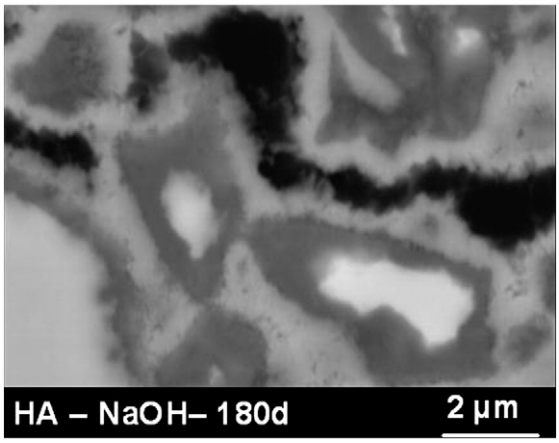

Fig. 5. Microstructure of NaOH activated HA slag after 180 days showing the presence of 2 types of C-S-H, a dark one with high Na content and a bright one with relatively low Na content.

higher sodium content is observed. The increase in alkali content of the C-N-S-H may be also related to a more porous C-S-H with similar composition; rich in NaOH-filled pores where the alkalis have precipitated (as NaOH or as a carbonate phase) when the samples were dried prior to analysis. However, the solvent exchange applied to stop the hydration and the high porosity exhibited by the samples activated using NaOH makes this suggestion less plausible than an incorporation of the Na in the C-S-H phases. It seems that the presence of Na in the C-N-S-H does not modify the aluminium uptake or the Ca/Si ratio. The formation of a second type of C-S-H (C-N-S-H) in the NaOH activated slags is consistent with the presence of two types of C-S-H observed in these samples by XRD (Fig. 3). The continuous increase of the basal peak on the XRD analysis is consistent with the continuous growth of the inner dark C-N-S-H layer observed in SEM images. This suggests that the basal peak observed in this study may be related to the inner C-N-S-H observed and is confirmed by the NSH_5 results where nor basal peak was observed neither inner C-N-S-H layer in the SEM images.

The Si, Mg, and Al contents were used to plot the Mg/Si vs. Al/Si ratios (Fig. 8) as described by Taylor et al. [8]. The good correlation of Mg/Si with Al/Si indicates the presence of a hydrotalcite like phase, while the presence of a positive x-axis intercept reveals the level of incorporation of Al in the C-S-H. The Mg/Al molar ratio is almost constant in all samples with a mean value of 2.1. This Mg/Al ratio is well within the range reported 1.92 to 4.35 for hydrotalcite formed in hydrated slag pastes [15,42].

The higher amount of Al_2O_3 in the HA slag leads to a higher amount of Al taken up by C-S-H (Al/Si = 0.23) than observed for the LA slag (Al/Si = 0.13), but does not change the composition of the hydrotalcite.

3.4. Microstructural changes

3.4.1. Microstructural development

Fig. 6 shows backscattered SEM images of the microstructure of the two slags after 28 days activated by NaOH and NSH_5. The reacting slag grains are surrounded by C-S-H rims. The C-S-H developed in the NaOH activated slags exhibits a brighter grey level than the C-S-H in the NSH_5 activated systems. As a constant chemical composition of the C-S-H with a Ca/Si from 0.8 to 0.9 was observed, the increased brightness indicates a higher density and/or a reduced amount of chemical bound water in the C-S-H of the NaOH activated slag.

The thickness of the C-S-H layers seems to be much lower for the samples activated using NaOH, and more pores are visible in the matrix. This may be due to the faster reaction of the slag in the case of NaOH activator that leads to a fast precipitation of relatively dense

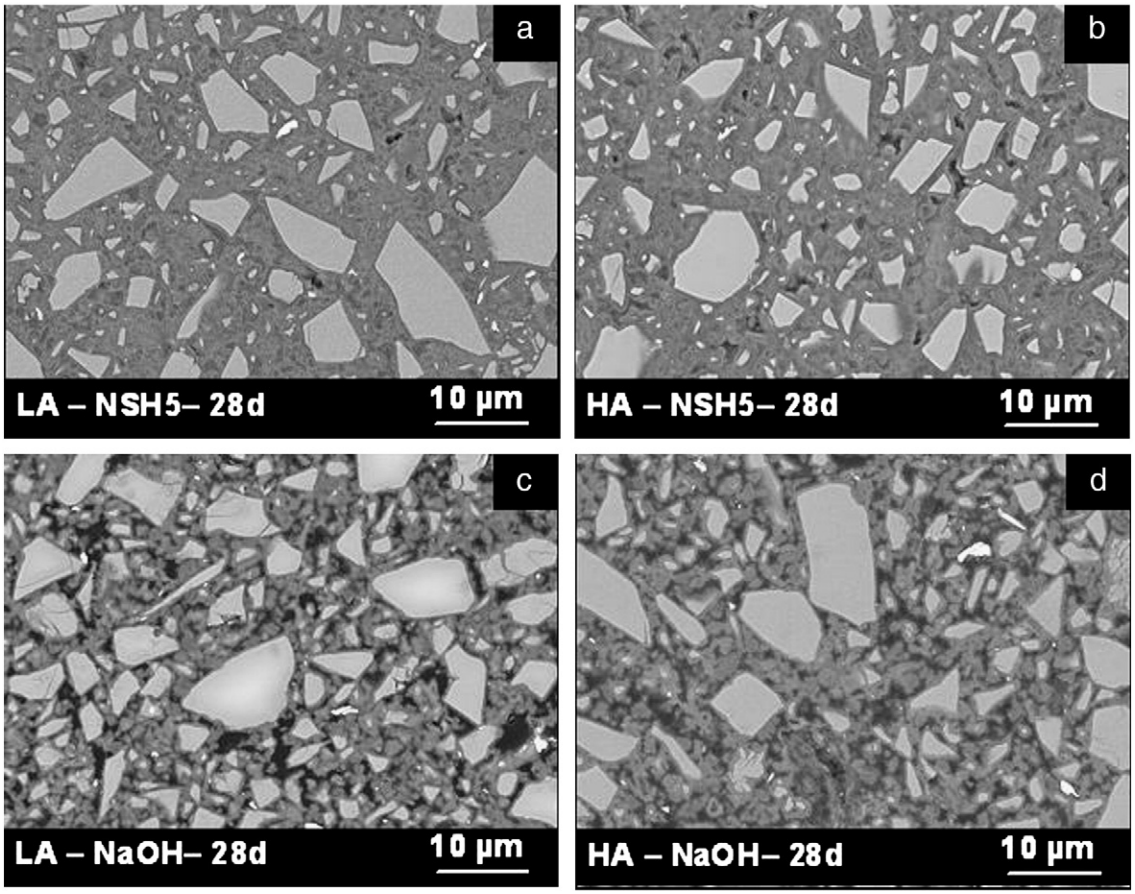

Fig. 6. Microstructure after 28 days for the different slags using the different activators. (a) LA slag with NSH_5 after 28 days, (b) HA slag with NSH_5 after 28 days, (c) LA slag with NaOH after 28 days, and (d) HA slag with NaOH after 28 days.

hydrates during the first day around the slag particles as shown in Fig. 4. Further hydrates develop almost entirely in the place of the original slag particles (analogous to inner C-S-H in cement hydration), with very little formation in the empty pore space. The microstructure remains coarser and the hydration products are less homogeneously distributed in the matrix even after 180 days (Fig. 5). Two types of C-S-H phases seem to have formed in the NaOH system: a dense C-S-H at early age of hydration and a less dense C-N-S-H at later ages (darker inner area in Fig. 5), containing more Na.

The BSE image of the NaOH activated slag systems after 1 day of hydration shows a C-S-H layer precipitating around the slag particles with some platelets of the hydrotalcite phase (see Fig. 4) in the matrix as shown by the EDX points analysis (Fig. 8). In case of the HA slag, more and larger platelets seem to be present after 1 day compared to LA slag. These platelets observed at an early age appear to be interlocked, and the space between those has been filled with C-S-H. In the case of the NSH_5 activator, almost no hydration products are observed after one day. At later ages, hydrotalcite formation has been observed mainly around the slag grains.

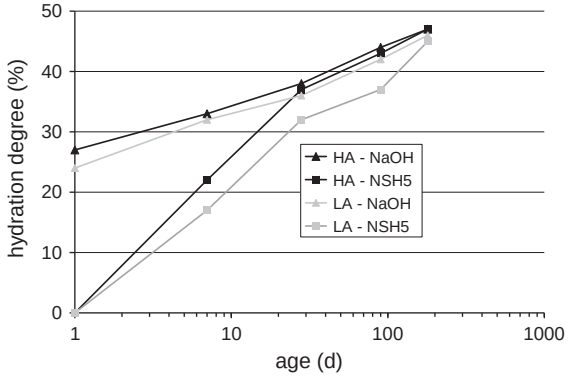

Fig. 7. Evolution of the hydration degree in % of the alkali activated slags as measured by SEM-IA (measurement uncertainty 2–3%).

3.4.2. Degree of reaction measured by SEM-IA

Up to 7 days, a much faster reaction of the slag in the NaOH activated system than in the NSH_5 activated system is observed (Table 6 and Fig. 7). However, after 28 days, no significant differences between the two activators occur. In all pastes, around 50% of the slag has hydrated after 180 days. Thus, the initial fast reaction of the NaOH activated slags and the rapid formation of a hydration layer seem not to prevent further hydration of the slag grains. Indeed, SEM-IA as well as microstructure observations showed clearly continuous consumption of the slag particles and the continuous formation and increase of the inner C-S-H layer. This is comparable to what is observed with temperature effect on OPC hydration where a fast reaction is leading to the formation of a thick hydration layer around the OPC. However, this layer does not prevent the late reaction of OPC.

Comparison of the SEM-IA results with the thermogravimetry data (see Fig. 9) indicates a higher amount of bound water after 90 and 180 days of the NSH_5 than of the NaOH activated samples, while the degree of reaction by SEM-IA of the anhydrous slag is similar. This discrepancy indicates the presence of different hydrates or hydrates with a different water content in the NSH_5 and NaOH activated slags.

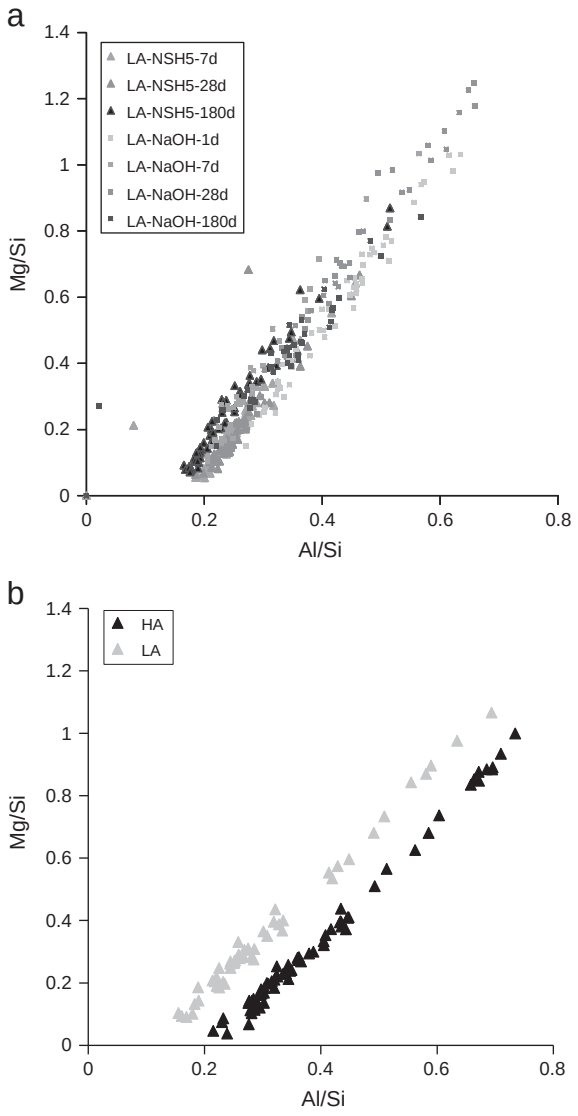

Fig. 8. Atomic ratios Mg/Si vs. Al/Si of (a) GGBFS LA using both activators at different ages and (b) comparison between both slags using NaOH at 28 days.

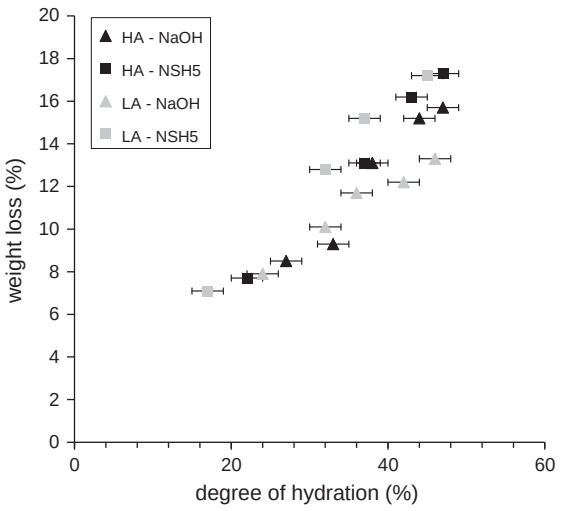

Fig. 9. Comparison between degree of hydration and weight loss for all activated systems.

This is also in agreement with the XRD data which seem to show some differences as well.

HA slag appears to show slightly faster reaction kinetics than LA slag, especially for NSH_5 at sample ages up to 28 days. Although, the chemical bound water of LA and HA were very similar.

3.4.3. Coarse porosity

The main reduction in coarse porosity as determined by SEM-IA (Table 7) of the NaOH activated slags takes place within the first day, from about 55 vol.% (space occupied by water and air during the mixing process) to about 19 vol.%. After the first day, the reduction in the coarse porosity proceeds very slow in NaOH activated slags. The diameter of pores with NaOH activator can reach up to 5 μm and even after 180 days, these pores do not seem to be filled with hydrates.

Because of the slow initial rate of reaction, samples activated with NSH_5 have a higher coarse porosity at a very early age. After 7 days and longer, the porosity becomes lower for these samples, and the pore space is gradually filled. For NSH_5 activated slags, the coarse pores become finer with time, as the contacts and bonds between hydration products develop (see Fig. 6).

With NaOH as activator, both slags show almost no significant difference in the development of coarse porosity with hydration time. With NSH_5, the coarse porosity decreases faster in the HA system, which is consistent with the faster hydration kinetics (see Table 6).

3.5. Discussions

3.5.1. Microstructure

The Al_2O_3 content influences both the morphology of C-S-H and the microstructure at 1 day of hydration in NaOH activated systems (Fig. 4). At an early age, the C-S-H of the LA slag appears to be more fibrous and the hydrotalcite platelets are smaller. The C-S-H particles of HA are more closely packed. However, at later ages the microstructure of both systems collapses towards a denser and more stable configuration with fewer large gel pores. The microstructural development showed in both cases the rims of C-S-H surrounding the larger slag particles. The C-S-H typically has a two-tone appearance and the layer formed later is darker than the layer formed earlier. The difference is attributed to different nanoporosities and therefore to different densities and backscattered electron coefficients. The main differences observed between the two different slags containing 7 and 12% of Al_2O_3 at later ages are the increased Al-

Table 6
Degree of reaction in % of the alkali activated slags as measured by SEM-IA. Measurement uncertainty 2–3%.

Age (day)	HA		LA	
	NaOH	NSH_5	NaOH	NSH_5
1	27	–	24	–
7	33	22	32	17
28	38	37	36	32
90	44	43	42	37
180	47	47	46	45

Table 7
Coarse porosity in vol.% of the alkali activated slags as measured by SEM-IA.

Age (day)	HA		LA	
	NaOH	NSH_5	NaOH	NSH_5
1	20	–	19	–
7	15	13	15	15
28	15	6	14	9
90	14	3	13	4
180	13	1	13	2

content of the C-S-H for the HA and the faster reaction HA compared to LA slag at an early age.

It was suggested previously [14,42,44] that the C-S-H gels present in commercial blast-furnace slag activated by KOH are related by both composition and morphology to the C-S-H gels present in slag-OPC pastes but are more crystalline. The same observations concerning the inner product C-S-H were made. It was shown its intermix on a fine scale with a Mg,Al-rich phase with similar Mg/Al ratio as observed here. The current work based on the results of NaOH activated slag gives further support. The data produced by both SEM and XRD indicated a structure based on a tobermorite-like phase as suggested by Taylor [45] with higher incorporation of alkali in the C-S-H. However, a study on KOH activated slags [14] indicated that more alkali (K^+) were binding in the silicate chains in the outer product than the inner product, while in the present NaOH activated systems, more Na^+ was bound in the inner product than the outer.

3.5.2. Hydration mechanisms

For both activators and slags, the hydration reactions are comparable: they both react to form C-S-H and hydrotalcite like phase. There are however several important differences: In comparison to the NSH_5 system, the NaOH activated system exhibits

(i) a faster decrease of coarse porosity and reaction kinetics during the first days of hydration,
(ii) a more crystalline type of C-S-H is observed by XRD,
(iii) the hydrotalcite forms larger crystals although its chemical composition is similar in both systems,
(iv) a higher coarse porosity for similar hydration degree
(v) a lower volume of hydration products and amount of bound water,
(vi) a lower compressive strength for similar hydration degree.

The fast initial reaction of the NaOH activated slag seems to result in the formation of a denser C-S-H with less chemically bound water and thus an increased coarse porosity at later ages (Figs. 5 and 6) resulting in a lower compressive strength as shown in Fig. 11. The high initial rate of reaction does not allow time for diffusion and therefore a high concentration of hydration products is built up in the zone immediately surrounding the hydrating slag grains. As slag dissolution continues, further hydrates are formed mainly in the place of the original slag particle but not in the empty coarse pores. Thus, the initial fast reaction seems to be responsible for the resulting coarse porosity and the low compressive strength at longer hydration times. The mechanism seems to be similar to the coarsening of the microstructure that is observed for OPC hydrated at elevated temperatures [24,25]. As for OPC systems at higher temperatures, a fast initial reaction seems to result in a dense hydrate layer, in a less well developed microstructure, in higher coarse porosity and thus in lower mechanical properties at later ages. A similar coarsening is also observed in alkali-activated fly ash and metakaolin binders, which has been attributed to differences in gel crosslinking and density [43].

3.5.3. Effect of microstructure on compressive strength

With both activators, compressive strength increases uniformly with the degree of hydration as shown in Fig. 10. However, at the same degree of hydration, the compressive strength is lower for NaOH activated systems compared to those activated by NSH_5. Both slags show, when activated with the same activator, the same correlation between compressive strength and hydration degree.

NaOH activated systems exhibited a microstructure comprising clustered dense particulates with large interconnected pores observed by SEM while the samples hydrated using NSH_5 appear homogeneous with porosity distributed in small pores largely below the observation limits in SEM micrographs. The fast reaction in the NaOH activated slag may allow an extensive gel organization and densification as observed in the temperature studies as well as for geopolymers [43,46], and thus results in a microstructure comprising dense gel particles and large interconnecting pores. In contrast, reduced reaction rates promote a decreased localized gel density and a well distributed porosity.

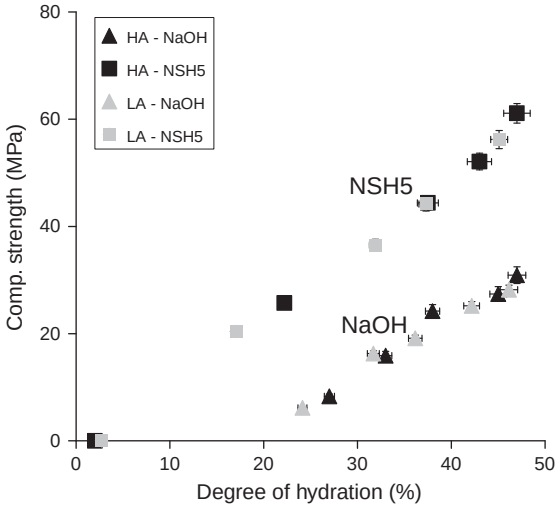

Fig. 10. Compressive strength vs. degree of hydration measured by SEM-IA.

The increase in gel volume allows supporting the compressive strength of NSH_5 activated slag. Therefore, an increase in strength is mainly a product of increased homogeneity of the microstructure. The slow increase in long term compressive strength of NaOH activated systems is not related to more unreacted material left since the same hydration degree is observed at later ages for both systems.

A comparison of the compressive strength with the measured coarse porosity (Fig. 11) shows a clear negative correlation with no significant differences between the two types of activators or the slag used. The differences in the correlation of the compressive strength with the degree of reaction and the coarse porosity imply that products formed in the NaOH activated samples have different space filling properties.

Since the C-S-H formed using NaOH at early ages is denser and less porous, the space in the matrix is poorly filled by the outer hydration products which consequently leads to lower compressive strength at the same degree of slag reaction compared to the NSH_5 activated samples. Therefore, to achieve a cementitious binder with high strength, an intrinsically more voluminous porous gel microstructure is required as suggested by investigations on geopolymers [43].

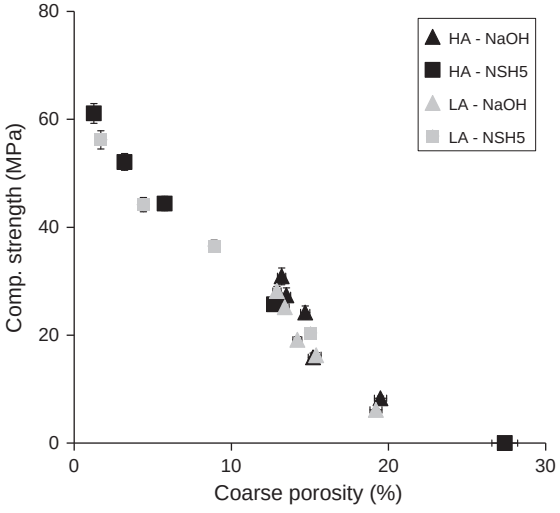

Fig. 11. Compressive strength vs. coarse porosity measured by SEM-IA.

3.5.4. Degree of hydration

In this study, the degree of reaction of alkali activated slags is measured using SEM image analysis [29], by comparing the volume of anhydrous slag with the original slag content in slag pastes. During the first days, a faster hydration was observed for NaOH activated samples, while at later ages the degree of hydration is similar regardless of the activator used. This observation agrees with other findings on alkali activated slag [36], where it was observed using selective dissolution techniques that more slag reacts in the presence of NaOH than of NSH_5, but the content of non evaporable water does not show a difference. This discrepancy was attributed to the fact that NSH_5 activated slag formed a water-bearing gel which was not observed by the techniques used in that study.

Within the studied alkaline solutions, it is shown that the ultimate degree of reaction of slags is not limited by fast early age reaction (NaOH activated systems). The content of the chemically bound water (or non-evaporable water) to measure the degree of hydration was adopted previously in different cementitious composites by comparing the quantity at different ages to the ultimate bound water (or non-evaporable water) at 100% degree of hydration. However it appears that this method cannot provide the real degree of hydration when the kinetics of reaction are different. The chemically bound water in C-S-H appears to decrease as reaction rate increases. Therefore, the ultimate chemically bound water should be much less. The degree of hydration calculated from constant chemically bound water cannot reflect real values, it is in fact, much lower than real degree of hydration (Fig. 9).

Fast reaction may increase the density of C-S-H leading to a decrease in the gel porosity. The diffusion of water continues, which consequently leads to the continuous formation of larger quantity of inner C-S-H instead of outer C-S-H. This can be concluded from the continuous increase in inner C-S-H thickness and almost no filling in capillary porosity for the NaOH activated systems after 7 days.

The density of C-S-H under saturated conditions is related to the gel porosity and composition. The results from EDS analysis show that the $Ca/(Al+Si)$ is constant regardless of the activator. Thus, the density of C-S-H is related only to the chemically bound water and gel porosity.

It is known that the bound water in C-S-H is present as both H_2O molecule and OH. Fast reaction may increase the polymerization of silicate chains and therefore part of water in the form of OH is lost due to a condensation reaction. However, this cannot influence a lot the density of C-S-H because most of the water exists in the form of interlayer water as shown for high temperature studies [47]. Thus, when fast kinetics occurs in the systems, less water may exist in the interlayer leading to a lower interlayer space and therefore a higher density.

It is concluded that the measurement of the amount of bound water is an inadequate method to compare indirectly the reaction degree of the slag in the presence of different alkaline activators. In the present study, image analysis is used to determine the degree of slag reaction. As we found as well a discrepancy between bound water content and direct measurement of slag hydration degree by SEM-IA, one can conclude that the C-S-H resulting from NaOH activated slag seems to incorporate less water than the one resulting from NSH_5 activated systems.

4. Conclusions

The investigated alkaline activators NaOH and sodium metasilicate pentahydrate (NSH_5) have a strong impact on microstructure and compressive strength of slag based binders by influencing the hydration kinetics, porosity and hydration products. Two slags with different Al_2O_3 contents (7 wt.% and 12 wt.%) are used in this study. In all systems, a C-S-H incorporating aluminium and a hydrotalcite phase are the main hydration products.

Clear differences are observed between the NaOH and the NSH_5 activator. The initial rate of reaction is higher using NaOH. During the fast initial hydration reaction a dense C-S-H with, compared to the NSH_5 activated system, less chemically bound water is formed, the microstructure is coarser, and the hydration products appear not well distributed throughout the matrix. During the late hydration of the NaOH activated slags, despite the continuous reaction, the increase in compressive strength and the decrease of coarse porosity is limited. The late C-S-H formed has a higher alkali incorporation and is easily distinguishable from the C-S-H formed earlier by scanning electron microscopy.

In the NSH_5 activated system, the slag hydrates slowly and there is ample time for the hydration products to diffuse and precipitate relatively uniformly throughout the interstitial space between the slag grains. This results in a lower porosity and much higher compressive strength at the same degree of slag reaction compared to the NaOH activated system.

The slag with higher Al_2O_3 content (12 wt.%) shows a slightly faster reaction kinetic than the slag with lower Al_2O_3 content (7 wt.%), but in both slags a C-S-H incorporating Al and a hydrotalcite phase are the main hydration products. In the case of the slag with higher Al_2O_3 content a higher Al uptake by the C-S-H is observed.

It appears that the chemical composition of the slag, in this case the Al content, has much less influence on hydration kinetics, nature of hydration products and strength development than a change of the alkaline activator.

Acknowledgements

The authors would like to acknowledge Walter Trindler and Boris Ingold for their help with the experimental work. The authors would like to acknowledge also the anonymous reviewers that improved the quality of the paper with their helpful comments.

References

[1] E. Gartner, Industrially interesting approaches to "low-CO_2" cements, Cement and Concrete Research 34 (2004) 1489–1498.
[2] M.C.G. Juenger, F. Winnefeld, J.L. Provis, J.H. Ideker, Advances in alternative cementitious binders, Cement and Concrete Research (in press), doi:10.1016/j.cemconres.2010.11.012.
[3] J. Davidovits, Geopolymers and geopolymeric materials, Journal of Thermal Analysis and Calorimetry 35 (1989) 429–441.
[4] P. Duxson, A. Fernández-Jiménez, J. Provis, G. Lukey, A. Palomo, J. van Deventer, Geopolymer technology: the current state of the art, Journal of Materials Science 42 (2007) 2917–2933.
[5] P. Duxson, J.L. Provis, G.C. Lukey, J.S.J. van Deventer, The role of inorganic polymer technology in the development of 'green concrete', Cement and Concrete Research 37 (2007) 1590–1597.
[6] V.D. Glukhovsky, G.S. Rostovskaja, G.V. Rumyna, High strength slag-alkaline cements, 7th International Congress on the Chemistry of Cements, Paris, France, 1980, pp. V164–V175.
[7] S. Caijun, L. Yinyu, Investigation on some factors affecting the characteristics of alkali-phosphorus slag cement, Cement and Concrete Research 19 (1989) 527–533.
[8] H.F.W. Taylor, Cement Chemistry, in: A.S.o.C. Engineers (Ed.), Second Edition, 1997, pp. 480 pages.
[9] D.M.R. Brew, F.P. Glasser, The magnesia-silica gel phase in slag cements: alkali (K, Cs) sorption potential of synthetic gels, Cement and Concrete Research 35 (2005) 77–83.
[10] A. Gruskovnjak, B. Lothenbach, L. Holzer, R. Figi, F. Winnefeld, Hydration of alkali-activated slag: comparison with ordinary Portland cement, Advances in Cement Research 18 (2006) 119–128.
[11] I.G. Richardson, The calcium silicate hydrates, Cement and Concrete Research 38 (2008) 137–158.
[12] S.-D. Wang, K.L. Scrivener, Hydration products of alkali activated slag cement, Cement and Concrete Research 25 (1995) 561–571.
[13] C.K. Yip, G.C. Lukey, J.S.J. van Deventer, The coexistence of geopolymeric gel and calcium silicate hydrate at the early stage of alkaline activation, Cement and Concrete Research 35 (2005) 1688–1697.
[14] I.G. Richardson, A.R. Brough, G.W. Groves, C.M. Dobson, The characterization of hardened alkali-activated blast-furnace slag pastes and the nature of the calcium silicate hydrate (C-S-H) phase, Cement and Concrete Research 24 (1994) 813–829.

[15] S.-D. Wang, K.L. Scrivener, 29Si and 27Al NMR study of alkali-activated slag, Cement and Concrete Research 33 (2003) 769–774.
[16] A. Fernandez-Jimenez, F. Puertas, Effect of activator mix on the hydration and strength behaviour of alkali-activated slag cements, Advances in Cement Research 15 (2003) 129–136.
[17] F. Puertas, A. Fernández-Jiménez, M.T. Blanco-Varela, Pore solution in alkali-activated slag cement pastes. Relation to the composition and structure of calcium silicate hydrate, Cement and Concrete Research 34 (2004) 139–148.
[18] A. Roy, P.J. Schilling, H.C. Eaton, P.G. Malone, W.N. Brabston, L.D. Wakeley, Activation of ground blast-furnace slag by alkali-metal and alkaline-earth hydroxides, Journal of the American Ceramic Society 75 (1992) 3233–3240.
[19] S. Song, H.M. Jennings, Pore solution chemistry of alkali-activated ground granulated blast-furnace slag, Cement and Concrete Research 29 (1999) 159–170.
[20] V. Zivica, Effects of type and dosage of alkaline activator and temperature on the properties of alkali-activated slag mixtures, Construction and Building Materials 21 (2007) 1463–1469.
[21] S.-D. Wang, K.L. Scrivener, P.L. Pratt, Factors affecting the strength of alkali-activated slag, Cement and Concrete Research 24 (1994) 1033–1043.
[22] A. Fernández-Jiménez, J.G. Palomo, F. Puertas, Alkali-activated slag mortars: mechanical strength behaviour, Cement and Concrete Research 29 (1999) 1313–1321.
[23] A. Fernández-Jiménez, F. Puertas, Setting of alkali-activated slag cement: influence of activator nature, Advances in Cement Research 13 (2001) 115–121.
[24] K.O. Kjellsen, R.J. Detwiler, O.E. Gjorv, Pore structure of plain cement pastes hydrated at different temperatures, Cement and Concrete Research 20 (1990) 927–933.
[25] J.I. Escalante-García, J.H. Sharp, The microstructure and mechanical properties of blended cements hydrated at various temperatures, Cement and Concrete Research 31 (2001) 695–702.
[26] R.L. Snyder, D.L. Bish, Quantitative analysis, in: D.L. Bish, J.E. Post (Eds.), Modern Powder Diffraction, Reviews in Mineralogy, 20, Mineralogical Society of America, 1989.
[27] M. Ben Haha, Mechanical effects of alkali silica reaction in concrete studied by SEM-image analysis, Materials department, EPFL, Lausanne, 2006, pp. 232.
[28] M. Ben Haha, E. Gallucci, A. Guidoum, K.L. Scrivener, Relation of expansion due to alkali silica reaction to the degree of reaction measured by SEM image analysis, Cement and Concrete Research 37 (2007) 1206–1214.
[29] M. Ben Haha, K. De Weerdt, B. Lothenbach, Quantification of the degree of reaction of fly ash, Cement and Concrete Research 40 (2010) 1620–1629.
[30] K.L. Scrivener, Backscattered electron imaging of cementitious microstructures: understanding and quantification, Cement and Concrete Composites 26 (2004) 935–945.
[31] K.L. Scrivener, T. Füllmann, E. Gallucci, G. Walenta, E. Bermejo, Quantitative study of Portland cement hydration by X-ray diffraction/Rietveld analysis and independent methods, Cement and Concrete Research 34 (2004) 1541–1547.
[32] E. Kanezaki, Thermal behavior of the hydrotalcite-like layered structure of Mg and Al-layered double hydroxides with interlayer carbonate by means of in situ powder HTXRD and DTA/TG, Solid State Ionics 106 (1998) 279–284.
[33] K. Rozov, U. Berner, C. Taviot-Gueho, F. Leroux, G. Renaudin, D. Kulik, L.W. Diamond, Synthesis and characterization of the LDH hydrotalcite–pyroaurite solid-solution series, Cement and Concrete Research 40 (2010) 1248–1254.
[34] B. Lothenbach, A. Gruskovnjak, Hydration of alkali-activated slag: thermodynamic modelling, Advances in Cement Research 19 (2007) 81–92.
[35] F. Puertas, A. Fernández-Jiménez, Mineralogical and microstructural characterisation of alkali-activated fly ash/slag pastes, Cement and Concrete Composites 25 (2003) 287–292.
[36] J.I. Escalante-Garcia, A.F. Fuentes, A. Gorokhovsky, P.E. Fraire-Luna, G. Mendoza-Suarez, Hydration products and reactivity of blast-furnace slag activated by various alkalis, Journal of the American Ceramic Society 86 (2003) 2148–2153.
[37] A. Gruskovnjak, B. Lothenbach, F. Winnefeld, B. Münch, R. Figi, S. Ko, M. Adler, U. Mäder, Quantification of hydration phases in supersulphated cements : review and new approaches, Advances in Cement Research (accepted).
[38] G. Renaudin, J. Russias, F. Leroux, F. Frizon, C. Cau-dit-Coumes, Structural characterization of C-S-H and C-A-S-H samples—part I: long-range order investigated by Rietveld analyses, Journal of Solid State Chemistry 182 (2009) 3312–3319.
[39] K. Garbev, B. Günter, M. Bornefeld, L. Black, P. Stemmermann, Cell dimensions and composition of nanocrystalline calcium silicate hydrate solid solutions. Part 1: synchrotron-based X-ray diffraction, Journal of the American Ceramic Society 91 (2008) 3005–3014.
[40] X. Hou, R.J. Kirkpatrick, L.J. Struble, P.J.M. Monteiro, Structural investigations of alkali silicate gels, Journal of the American Ceramic Society 88 (2005) 943–949.
[41] F. Puertas, A. Fernandez-Jimenez, M.T. Blanco-Varela, Pore solution in alkali-activated slag cement pastes. Relation to the composition and structure of calcium silicate hydrate, Cement and Concrete Research 34 (2004) 139–148.
[42] I.G. Richardson, Tobermorite/jennite- and tobermorite/calcium hydroxide-based models for the structure of C-S-H: applicability to hardened pastes of tricalcium silicate, [beta]-dicalcium silicate, Portland cement, and blends of Portland cement with blast-furnace slag, metakaolin, or silica fume, Cement and Concrete Research 34 (2004) 1733–1777.
[43] P. Duxson, J.L. Provis, G.C. Lukey, S.W. Mallicoat, W.M. Kriven, J.S.J. van Deventer, Understanding the relationship between geopolymer composition, microstructure and mechanical properties, Colloids and Surfaces A: Physicochemical and Engineering Aspects 269 (2005) 47–58.
[44] I.G. Richardson, The nature of the hydration products in hardened cement pastes, Cement and Concrete Composites 22 (2000) 97–113.
[45] H.F. Taylor, Proposed structure for calcium silicate hydrate gel, Journal of the American Ceramic Society 69 (1986) 464–467.
[46] C. Famy, K.L. Scrivener, A. Atkinson, A.R. Brough, Effects of an early or a late heat treatment on the microstructure and composition of inner C-S-H products of Portland cement mortars, Cement and Concrete Research 32 (2002) 269–278.
[47] X. Cong, R.J. Kirkpatrick, Effects of the temperature and relative humidity on the structure of C-S-H gel, Cement and Concrete Research 25 (1995) 1237.